ARTICLE

BIOTECHNOLOGY and BIOENGINEERING

Systems Analysis of Dynamic Transcription Factor Activity Identifies Targets for Treatment in Olaparib Resistant Cancer Cells

Joseph T. Decker,[1] Eric C. Hobson,[1] Yining Zhang,[2] Seungjin Shin,[3] Alexandra L. Thomas,[4] Jacqueline S. Jeruss,[4] Kelly B. Arnold,[1] Lonnie D. Shea[1]

[1]Department of Biomedical Engineering, University of Michigan, 2200 Bonisteel, 1119 Gerstacker, Ann Arbor 48109, Michigan; telephone: 734-764-7149; fax: 734-936-1905; e-mail: ldshea@umich.edu

[2]Department of Chemical Engineering, University of Michigan, Ann Arbor, Michigan

[3]Department of Chemical and Biological Engineering, Northwestern University, Evanston, Illinois

[4]Department of Surgery, University of Michigan, Ann Arbor, Michigan

ABSTRACT: The development of resistance to targeted therapeutics is a challenging issue for the treatment of cancer. Cancers that have mutations in BRCA, a DNA repair protein, have been treated with poly(ADP-ribose) polymerase (PARP) inhibitors, which target a second DNA repair mechanism with the aim of inducing synthetic lethality. While these inhibitors have shown promise clinically, the development of resistance can limit their effectiveness as a therapy. This study investigated mechanisms of resistance in BRCA-mutated cancer cells (HCC1937) to Olaparib (AZD2281) using TRACER, a technique for measuring dynamics of transcription factor (TF) activity in living cells. TF activity was monitored in the parental HCC1937 cell line and two distinct resistant cell lines, one with restored wild-type BRCA1 and one with acquired resistance independent of BRCA1 for 48 h during treatment with Olaparib. Partial least squares discriminant analysis (PLSDA) was used to categorize the three cell types based on TF activity, and network analysis was used to investigate the mechanism of early response to Olaparib in the study cells. NOTCH signaling was identified as a common pathway linked to resistance in both Olaparib-resistant cell types. Western blotting confirmed upregulation of NOTCH protein, and sensitivity to Olaparib was restored through co-treatment with a gamma secretase inhibitor. The identification of NOTCH signaling as a common pathway contributing to PARP inhibitor resistance by TRACER indicates the efficacy of transcription factor dynamics in identifying targets for intervention in treatment-resistant cancer and provides a new method for determining effective strategies for directed chemotherapy.

Correspondence to: L.D. Shea
Contract grant sponsor: National Institute of Biomedical Imaging and Bioengineering
Contract grant number: RO1GM097220-05
Received 24 September 2016; Revision received 10 March 2017; Accepted 16 March 2017
Accepted manuscript online 21 March 2017;
Article first published online 18 May 2017 in Wiley Online Library (http://onlinelibrary.wiley.com/doi/10.1002/bit.26293/abstract).
DOI 10.1002/bit.26293

Biotechnol. Bioeng. 2017;114: 2085–2095.

KEYWORDS: PARP inhibitors; data-driven modeling; drug resistance

Introduction

The genes BRCA1/BRCA2 play major roles in the repair of DNA double-strand breaks (DSBs) by homologous recombination (HR). HR repairs DSBs that occur in the late S and G2 phase of the cell cycle and also has a key role in resolving DSBs that result from unrepaired single-strand breaks (SSB). As such, mutations in the BRCA genes lead to an increased risk of genetic mutation and the subsequent development of cancer. Women carrying a mutation in BRCA1 or BRCA2 have a lifetime risk of developing breast cancer of up to 80%, with a risk of developing ovarian cancer of approximately 50% (Ford et al., 1994; King et al., 2003). Breast cancer and ovarian cancer are often associated with mutations in BRCA, with many BRCA1-driven breast cancers also being triple negative for the estrogen, progesterone, and HER2/neu receptors (ER^-, PR^-, $HER2^-$) (Foulkes et al., 2010; Reis-Filho and Tutt, 2008). Targeted therapy for triple negative breast cancer (TNBC) is currently lacking, and as such much research is directed toward understanding and developing chemotherapeutics to target this disease subtype.

One therapy targeted to BRCA-mutated cancers is the use of poly(ADP-ribose) polymerase (PARP) inhibitors (Farmer et al., 2005; Rottenberg et al., 2008; Rouleau et al., 2010). PARP is an enzyme that plays an important role in the recognition and repair of single-strand DNA breaks through the base excision repair (BER) pathway. Targeting this mechanism with PARP1 inhibitors has shown preclinical efficacy in tumors with homologous DNA repair

defects, such as those arising in BRCA1 or BRCA2 mutation carriers with breast cancer and ovarian cancer (Bryant et al., 2005; Farmer et al., 2005). The mechanism by which PARP inhibition can promote cell death in BRCA-mutated cells is thought to be through synthetic lethality, defined as the co-occurrence of multiple genetic events that results in organismal or cellular death (Lord et al., 2015). The PARP inhibitor Olaparib (AZD2281) is a small-molecule that has shown efficacy in patients with germline BRCA mutations in clinical trials (Buege and Mahajan, 2015; Gelmon et al., 2011; Ledermann et al., 2012; Tutt et al., 2009). Olaparib was recently approved for use in late-stage ovarian cancers with deleterious germline BRCA mutations as a result of its efficacy in clinical trials (Kim et al., 2015). Despite the effectiveness of PARP inhibitors in the treatment of BRCA-mutated cancers, some patients do not respond, and others can develop resistance to the drug with prolonged treatment. The mechanisms governing lack of responsiveness or the development of resistance are thought to occur through alterations in the transcriptional network (Barber et al., 2013; Henneman et al., 2015; Jaspers et al., 2013; Johnson et al., 2013; Lord and Ashworth, 2013). Identification of these changes offers the opportunity to develop combination therapy strategies that can enhance the efficacy of PARP inhibitors while also preventing the development of resistance.

The objective of this study was to quantify the regulatory dynamics of breast cancer cells in response to Olaparib treatment using cells that are both sensitive and resistant to PARP inhibition. We applied a TRanscriptional Activity CEll aRray (TRACER) to measure the large-scale dynamic activity of multiple transcription factors (TFs) that occur in response to Olaparib treatment for multiple cell populations. TRACER is distinct from other high-throughput approaches that measure the abundance of mRNA or protein within cells, as the repeated measurement of activity for multiple TFs within the same cell populations enables monitoring of the cellular adaptation to the presence of the drug and provides information on active signaling pathways that enable resistance. We employed data-driven modeling (Arnold et al., 2015; Beste et al., 2014) approaches that enable evaluation of relationships between TFs, rather than separate treatment of individual TFs. Network analysis of TF activity provided a unique perspective for both identifying tumor cells that are likely to be resistant to standard therapies as well as suggesting alternative multivariate targets for combinatorial treatment. Identifying the mechanisms of PARP1 inhibition-mediated cell death and resistance development during treatment has the potential to identify new strategies to maximize drug efficacy, guide associated combinatorial therapeutics to avoid resistance, and identify biomarker signatures to identify patients that are sensitive to PARP1 inhibitors.

Materials and Methods

Cells and Reagents

HCC1937 (BRCA1-mutated) tumor cell line is derived from a type of human ductal carcinoma bearing a BRCA1 5382insC mutation in one allele and a deletion of the second allele. The BRCA1 protein in HCC1937 lacks the BRCA1C terminus, and extracts show very low levels of BRCA1 protein. The cells were stably transfected with either the wild-type BRCA1-expressing vector or the null vector so that two cell lines (BRCA1 wild-type and mutant-type) were established (kindly gifted by Dr. Vincent Cryns).

Cell Viability Assay

Cell viability was analyzed by MTS assay (Sigma, St. Louis, MO). Cells (1500–3000) were plated in each well of a 96-well tissue culture plate with 100 μL of medium. The next day, the medium was replaced with 100 μL of fresh medium containing 10 μM Olaparib or 0.5 μM gamma secretase inhibitor, as indicated, and the cells were grown for 7 days. Stock Olaparib and gamma secretase inhibitor were prepared in DMSO. At the end of the treatment period, 10 μL of MTS solution was added to each well, the cells were incubated at 37°C for 1–2 h, and absorbance was read at 490 nm. Data are presented as a percentage of the control cells cultivated under the same conditions or the absorbance of the wells.

Lentivirus

Lentivirus was produced by co-transfecting HEK-293T cells with previously described lentiviral packaging vectors (pMDL-GagPol, pRSV-Rev, pIVS-VSV-G) (Dull et al., 1998) and lentiviral vectors using JetPrime (Polyplus, Illkirch, France). After 48 h, supernatants were collected and cell debris was spun down and removed. Viruses were concentrated using PEG-it (Systems Biosciences, Palo Alto, CA) and re-suspended in phosphate buffered saline (PBS).

Establishment of Olaparib-Resistant Cell Line From BRCA1 Mutant Cells

Olaparib-resistant clones were established by means of long-term exposure to gradually increasing concentrations of Olaparib (0.2, 0.5, 1, 2, 5, 10 μM, 1 week in each treatment). The cells that survived in the final 10 μM concentration of Olaparib were serially diluted to single cells and enriched without Olaparib. After establishing the clones, the drug resistance was confirmed and clones were selected that had drug resistance similar to BRCA1 wild-type cells.

Reverse Transcription-PCR (RT-PCR)

RNA was prepared from 5×10^5 cells by use of the Absolutely RNA Microprep Kit (Stratagene, Santa Clara, CA). Before reverse transcription, 1 μg of RNA was treated with RNase free-DNase I. Purified RNA (0.5 μg) was reverse transcribed with random hexamers using the Superscript III first-strand synthesis system (Life Technologies, Carlsbad, CA). β-actin was used as an internal control. The cycling conditions were as follows: pre-treatment at 95°C for 15 s, then 40 cycles of denaturation at 95°C for 5 s, and extension at 60°C for 30 s. Relative gene expression was quantified using the comparative ΔCT (CT: cycle threshold) method.

Transcription Factor Activity Arrays

TF reporters consist of a specific TF response element (TRE) cloned upstream of a minimal thymidine kinase promoter driving the gene

for firefly luciferase (FLUC). Increased binding of TFs at the TRE results in increased luciferase production and a proportional increase in luminescence when an excess of substrate is added during imaging, thus providing a quantitative measure of relative transactivation. TF reporter specificity and sensitivity studies are referenced on the TRANSFAC database. Each lentiviral reporter consists of three or four repeats of a TF-specific binding element driving expression of firefly luciferase.

Dynamic TF activity was measured for three different populations of HCC1937 cells: parent HCC1937 cells with mutated BRCA1 ($BRCA1^{MT}$), HCC1937 cells with wild-type BRCA1 ($BRCA1^{WT}$), and HCC1937 cells with mutated BRCA1 that have been selected for resistance to Olaparib ($BRCA1^{MT/RES}$). Cells with mutated BRCA1 have impaired DNA repair and are thus sensitive to PARP inhibitors such as Olaparib. Activity was measured for 44 different factors over 2 days of treatment with 10 μM Olaparib. Measurements acquired at several time points (0, 2, 4, 6, 8, 24, 48 h) allowed both initial differences between cell types as well as differences in response to Olaparib treatment to be elucidated from the data.

All cell types were transduced with 10 MOI of each TF activity-reporting lentivirus. Transduced cells were then seeded on a 384-well plate with at least four replicates of each condition. Two days after cell seeding, luciferase activity was measured using an IVIS Lumina LTE camera system (Caliper Life Sciences, Hopkinton, MA). The 2-day period is sufficient time for ensuring lentiviral gene expression. After changing media, cells were treated with 10 μM of Olaparib, and the luciferase activity was measured for 2 days. TA lentivirus, which is composed of only minimal promoter of thymidine kinase, was used as a control. The luciferase activity from TA lentivirus transduced cells highly correlates to cell number over time. Thus, all other TF activity was normalized with respect to TA activity and represented by TF/TA ratio.

Western Blot Analysis

Total cell protein was extracted in boiling SDS sample buffer (2% SDS, 50 mmol/L Tris–HCl [pH 6.8], 10% glycerol, 0.002% bromophenol blue, and 6% 2-mercaptoethanol). Cell extracts were separated by SDS–PAGE, and the proteins were transferred to polyvinylidene difluoride membrane (Millipore, Billerica, MA). Western blots were blocked in TBS-T buffer (10 mmol/L Tris–HCl [pH 7.4], 150 mmol/L NaCl, and 0.05% [v/v] Tween 20) containing 5% nonfat dry milk and probed with primary antibody in blocking buffer at 4°C overnight. Blots were washed with TBS-T buffer and incubated with secondary antibodies diluted in TBS-T at room temperature. Primary antibodies of anti-NOTCH1 and anti-NOTCH3 were obtained from Santa Cruz Biotechnology (Dallas, TX).

PLSDA Analysis

Partial least squares discriminant analysis (PLSDA) was performed in order to identify patterns in TF activity that distinguish between cell types and treatments (Benedict and Lauffenburger, 2012). PLSDA reduces model dimensionality by calculating orthogonal latent variables (LV) that best differentiate between classes. Scores calculated for observations can be plotted on LVs to allow for visualization of classification in a scores plot. Associated latent variable loadings enable identification of TF activity patterns associated with classification. Two separate PLSDA models were generated in this study; one using only data from the initial time point (single time point) and one using measurements from multiple time points (combined time-course). PLSDA calculations were performed using the orthogonal PLSDA algorithm in PLS Toolbox (Eigenvector Research, Manson, WA). Cross-validation was performed using k-fold cross-validation with $k = 10$, dividing the dataset into 10 subsets and testing each subset individually with the remaining used for training. In addition to cross-validation, the model was further validated by a permutation test, in which the classification efficacy of the PLSDA model was compared to additional PLSDA models generated using randomly permuted class labels using a Student's t-test. This test allowed for confirmation that the classification between the assigned cell types was significantly more effective than classification between random groups (Westerhuis et al., 2008). A single time point model was created with all cell groups ($BRCA1^{MT}$, $BRCA1^{WT}$, and $BRCA1^{MT/RES}$) at the initial measurement time point (48 h after seeding and transfection). A combined time-course model was also created using all three cell groups at multiple time points after treatment with Olaparib. Variable importance in projection (VIP) scores were used to select variables that were most effective in separating classes, eliminating those that were either not helpful or were confounding. The VIP scores for the selected variables indicate the relative importance of each variable in modelling the variance seen in TF activity measurements, and accordingly the most important variable for explaining the variance (Chong and Jun, 2005). The 35 variables with the highest VIP scores were selected in order to keep dimensionality consistent between single time-point and combined time-course PLSDA models.

Statistical and Systems Analysis

TF activity levels were normalized to a TA reporter with the corresponding treatment. We performed background subtraction and loss normalization to correct for systematic noise. All normalized TF activity levels were $\log_2$ transformed. Results of experiments are presented as the mean ± standard deviation unless otherwise indicated. Differences in means were evaluated by fitting an empirical hierarchical Bayesian linear model using the *limma* R package (Smyth, 2005). P-values were adjusted using the false discovery rate correction (Benjamini and Hochberg, 1995). A P-value of <0.05 was considered to be statistically significant. Each individual 384-well plate included only a subset of the measured TFs, requiring the formation of simulated multivariate observations (containing every TF) for hierarchical clustering and PLSDA, which were generated by randomly sampling independent TF activity measurements from within each cell type. A total of 1000 simulated observations were generated for each cell type in order to form a stable distribution, without calculating all possible combinations ($>10^{48}$). Variables with more than 25% of activity measurements

below background were removed from analysis. Mean-centering and variance scaling were used to standardize all data prior to multivariate analysis.

Hierarchical clustering was used to identify differences in TF activity between cell groups in an unsupervised manner (Arnold et al., 2016). Clustering was performed using Matlab software (Mathworks, Natick, MA) with Pearson's correlation coefficient as a distance metric. The clustering results were visualized using the *clustergram* function to generate a heatmap of relative TF activity with dendrograms indicating clusters for both TFs and samples.

Network Analysis

Network analysis of TF activity measurements was carried out using NTRACER, as described previously (Bernabé et al., 2016; Weiss et al., 2014). Briefly, normalized activity measurements are mean-centered and an initial network topology inferred through several different techniques: linear methods (PLSR; [Mevik and Wehrens, 2007], similarity index [Siletz et al., 2013], linear ordinary differential equations based on TIGRESS [Haury et al., 2012]), and nonlinear methods (ARACNE [Margolin et al., 2006], CLR [Faith et al., 2007], MRNET [Meyer et al., 2007], dynamic random forest [Breiman, 2001]). A prior knowledge network curated from GENEGO, TRANSFAC, and IPA was also included in the model. CellNOptR (Terfve et al., 2012) was used to optimize the network architecture. A total of 500 runs was performed. Edge significance was determined by comparing the number of edge occurrences in the 500 optimized networks to 500 networks generated from permutation samples from the same data. A *P*-value of 10^{-6} was used for significance. Finally, features were selected from the top 10% of significant edges at each set of time points to ensure high-quality edge selection. Networks were visualized using the R package *iGraph* (Csardi and Nepusz, 2006).

Results

BRCA1-Mutated HCC1937 Cancer Cells Were Sensitive to PARP1 Inhibitor Olaparib

The sensitivity of BRCA1-mutated HCC1937 cells to the PARP1 inhibitor Olaparib (AZD2281) was initially investigated. $BRCA1^{WT}$ cells were resistant to 10 μM of Olaparib compared with $BRCA^{MT}$ cells, with a twofold increase in cell viability after 7 days as measured by MTS assay (Fig. 1). These data are consistent with the previous observation that Olaparib has a cytotoxic effect on BRCA-mutated cells.

Prolonged exposure of HCC1937 cells to increasing doses of Olaparib over a 6-week period led to the development of resistance at the therapeutic dose (Fig. 1). Previous reports suggested BRCA1-mutated cell lines may develop resistance to Olaparib or other PARP inhibitors through a secondary mutation to restore the wild-type BRCA1 protein (Lord and Ashworth, 2013). RG-PCR for BRCA1 in the resistant cells confirmed that the cells retained the truncated BRCA1 mutant that is present in the parental cell line, indicating that wild-type BRCA1 protein was not restored in these cells (Fig. S1).

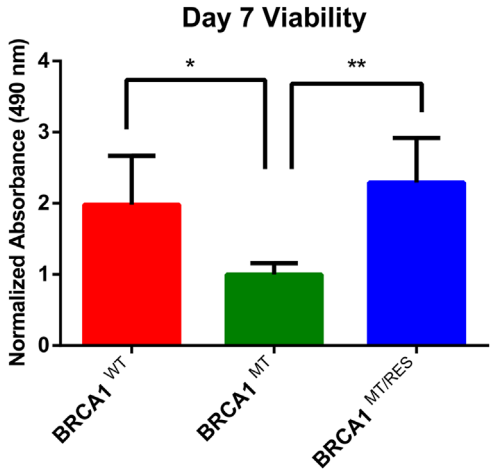

Figure 1. Cell viability after 7-day treatment with 10 μM Olaparib. Values are presented as absorbance at 490 nm normalized to the parental cell line. BRCA1WT and BRCA1MT/RES are both significantly different from BRCA1MT (* $P < 0.05$, ** $P < 0.01$).

Multivariate Analysis of TF Activity Before Treatment With Olaparib Predicted Phenotype and Provided Insight Into Systems-Level Mechanisms

TRACER was used to profile baseline (i.e., no drug treatment) differences in TF activity in the three cell types (Figs. 2 and S2). A total of 68% (30/44) of examined TFs were significantly different between $BRCA1^{WT}$ or $BRCA1^{MT/RES}$ cells and $BRCA^{MT}$ ($P < 0.05$). Of these factors, 10 were similar between $BRCA1^{WT}$ and $BRCA1^{MT/RES}$, 1 was significant in $BRCA1^{WT}$ only, and 19 were significant in $BRCA1^{MT/RES}$ only. The TFs that were common between $BRCA1^{WT}$ and $BRCA1^{MT/RES}$ suggested that there may be common mechanisms to producing resistance to Olaparib, while the TFs that were distinct between the two may suggest cell-type specific mechanisms.

Although univariate analysis may identify differences between cell groups based on the activity measurements of individual TFs, multivariate approaches allow for the identification of patterns in TF activity that can improve the classification and identifying relationships between TFs. We used hierarchical clustering to visualize multivariate differences in differentially active TFs in an unsupervised manner. Our results indicated distinct regulatory activity in $BRCA1^{MT}$, $BRCA1^{WT}$, and $BRCA1^{MT/RES}$ cells (Fig. 3). TFs associated with $BRCA1^{MT}$ cells include PTTG, E2F1, CRE, and STAT3, while HOXA1, STAT5, WT, and HIF1 were associated with $BRCA1^{WT}$ cells, and LHX8, IRF1, ISRE, SP1, RAR, SRF, and OCT4 were associated with $BRCA1^{MT/RES}$ cells. These TFs belong to a variety of pathways, including interferon response (IRF1 and ISRE), development (RAR, HOXA1, and LHX8), and pluripotency (OCT4).

PLSDA was used to identify linear combinations of TFs that best separated the three cell lines at single time points (Fig. S3A). PLSDA applied to TF activity data from all three cell types ($BRCA1^{MT}$, $BRCA1^{WT}$, and $BRCA1^{MT/RES}$) indicated separation between groups along two latent variables, with a calibration error ranging from 5.6% to 11.4% and a cross-validation error

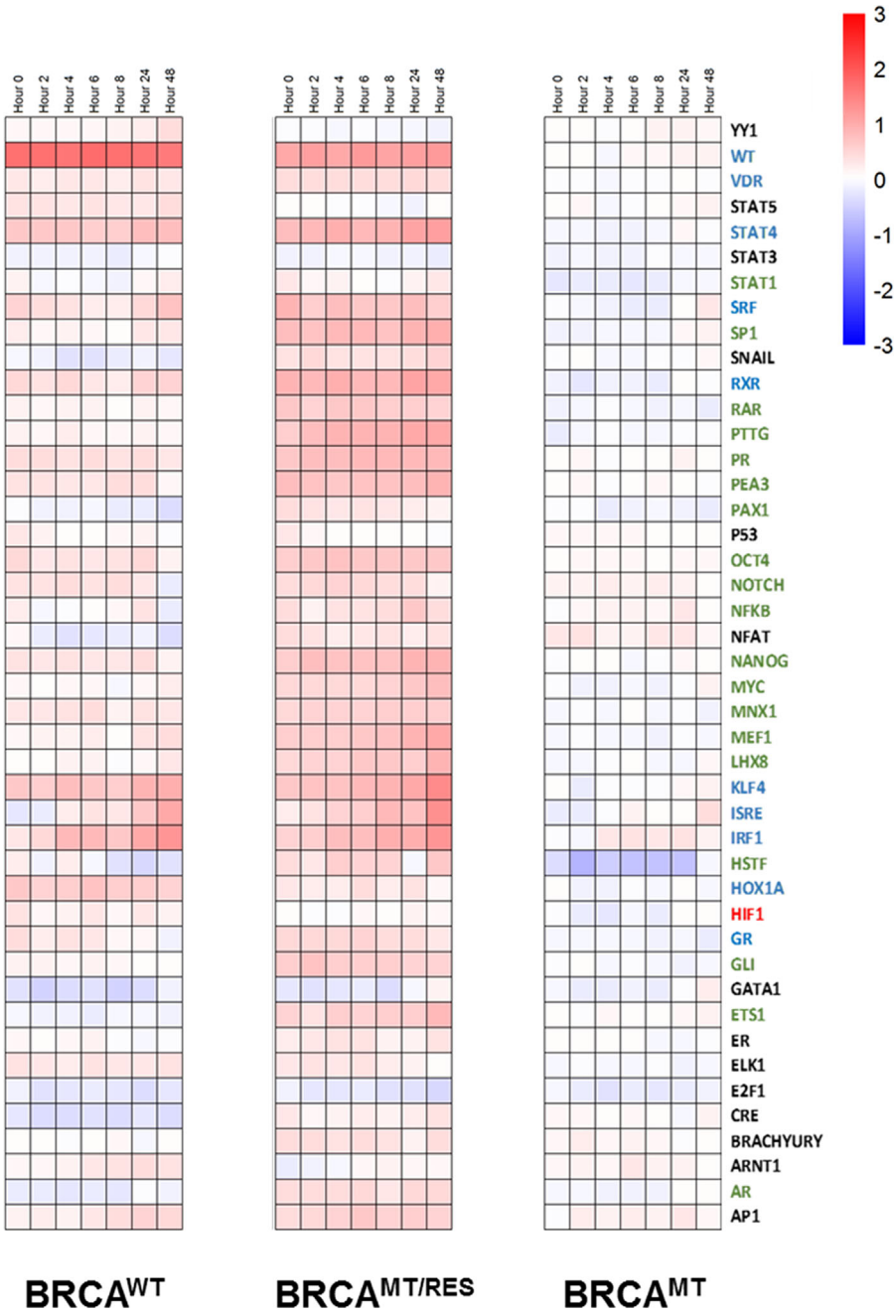

Figure 2. Dynamic transcription factor activity after treatment with Olaparib. Values are reported as $\log_2$ values for the treated condition normalized to the TA control reporter and untreated HCC1937 cells. Colors of TF names denote significance compared to $BRCA^{MT}$ during at least one measurement ($P < 0.05$). Red, $BRCA^{WT}$; Green, $BRCA^{MT/RES;}$ Blue, Both.

from 5.7% to 11.7% (Fig. S3B). In the PLSDA model of TF activity prior to Olaparib treatment (Time 0), the first latent variable separated $BRCA1^{WT}$ and $BRCA1^{MT}$ cells, while the second latent variable separated $BRCA1^{MT/RES}$ cells from the other types (Fig. 4A). $BRCA1^{MT}$ cells were scored negatively on LV1 and LV2 and, therefore, were associated with CRE, GATA1, E2F1, and PTTG. $BRCA1^{WT}$ cells, scored positively on LV1 and negatively on LV2, were associated with HIF1, STAT5, HOXA1, and WT, and $BRCA1^{MT/RES}$ cells, which scored positively on LV2, were associated with SP1, RAR, SRF, and OCT4 (Fig. 4B). Unsurprisingly, the TFs identified with each cell type using PLSDA were similar to those identified with hierarchical clustering. Of particular interest are TFs SRF, NOTCH, and OCT4 that are positively loaded on both LV1 and LV2, indicating association with both Olaparib resistant cell lines ($BRCA1^{WT}$ and $BRCA1^{MT/RES}$). Overall, PLSDA indicated that resistant cell phenotype can be predicted based on relationships between baseline TF activity measurements.

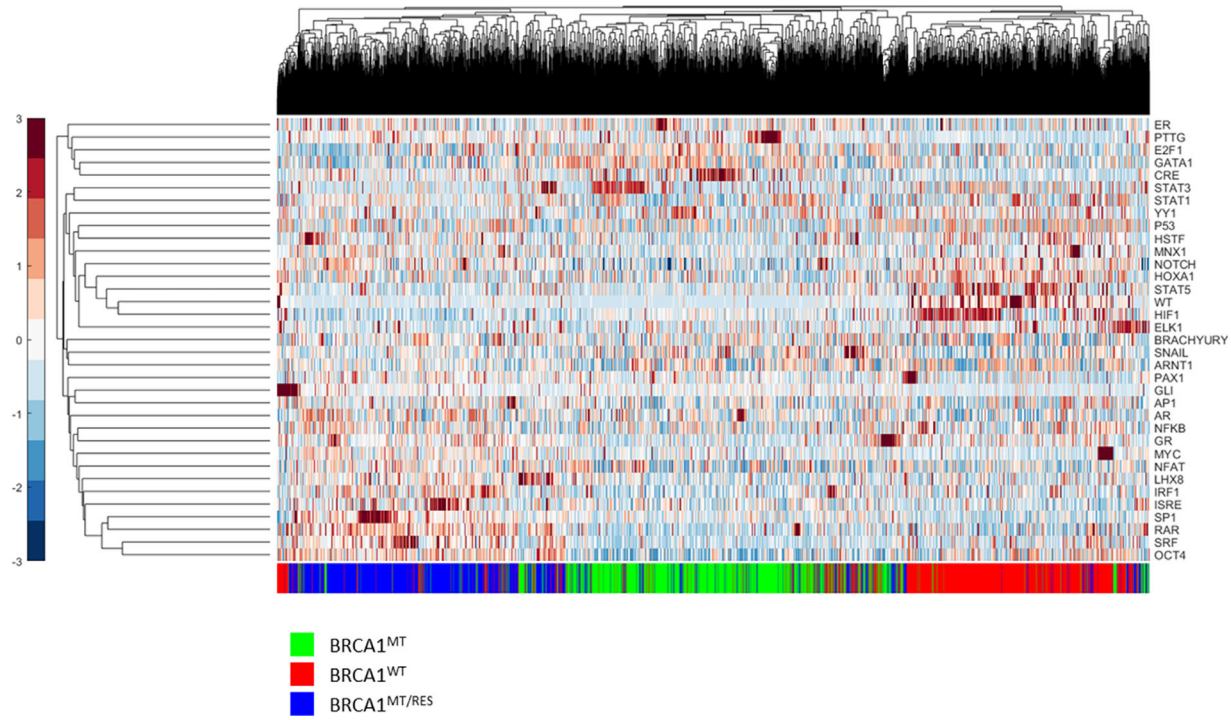

Figure 3. Unsupervised hierarchical cluster of bootstrapped multivariate observations based on transcriptional activity at the initial time point. $BRCA1^{MT}$ (BRCA1 mutant, green), $BRCA1^{WT}$ (BRCA1 wild-type, red), and $BRCA1^{MT/RES}$ cells (BRCA1 mutant with resistance to Olaparib, blue) were separated based on their transcriptional activity.

Measurements of Dynamic TF Activity Were More Predictive of Resistant Cell Phenotype and Gave Insight Into Temporal Patterns of TF Activation

Measurements from multiple time points were used to create a combined time-course PLSDA model using data collected before (Time 0) and after (Times 2–48) Olaparib treatment (Fig. 4C and D). We ensured the number of parameters was matched between combined time-course and single time point models by including only the top 35 parameters in the combined time-course model, as assessed by VIP scores. Interestingly, the model including temporal information was over 10-fold more accurate for differentiating cell phenotype (cross-validation error of 0.25%) (Fig. S3B), highlighting the importance of the ability to measure TF activity over time. PLSDA performed with permuted class labels performed with significantly worse CV accuracy ($P < 0.001$).

Examination of latent variable loadings revealed signatures of TF activation that may be useful in understanding differences in temporal signaling relationships based on cell phenotype (Fig. 4D). The first latent variable (LV) separated $BRCA1^{WT}$ and $BRCA1^{MT}$ cells, while the second LV distinguished $BRCA1^{MT/RES}$ cells (Fig. 4C). NOTCH activity measured 2 h after treatment was the most critical component of these signatures (as assessed by VIP score). The loadings for most TFs across time points remained similar, suggesting similar dynamic directionality. Intriguingly, however, NOTCH is loaded differently at each time point, indicating that there is a change in relative activity over the course of the experiment within different cell types. Two hours after treatment with Olaparib, NOTCH is loaded positively on both LV1 and LV2, associating it with the Olaparib-resistant cell types ($BRCA1^{WT}$ and $BRCA^{MT/RES}$). However, 48 h after treatment, NOTCH becomes more associated with the Olaparib-sensitive $BRCA1^{MT}$ cell type.

NOTCH as a Common Transcription Factor in Multiple Olaparib Resistance Mechanisms

Networks for TRACER (NTRACER) was used to identify relevant hubs of activity leading to resistance in $BRCA1^{WT}$ and $BRCA1^{MT/RES}$ cells (Fig. 5). These networks compared the differences in response between sensitive and resistant cell lines in order to identify differences in response that lead to the resistant phenotype. Specifically, the networks at the earliest time points (0–2 h, Fig. 5A and C) were examined to determine the initial effects of Olaparib treatment on the inferred dynamic regulatory network. NTRACER identified seven nodes directly connected to the $BRCA1^{MT/RES}$ cell type (PTTG, RAR, SP1, SRF, STAT1, AR, and HIF1), with five additional nodes (NOTCH, IRF1, GL1, SNAIL, and OCT4) regulated by one or more of the cell type-associated nodes. Similar connectivity was observed for $BRCA1^{WT}$ cells, with one node (Wilms tumor [WT]) associated with the cell type and four additional nodes (NOTCH, STAT5, HOX1A, and GL1) downstream of the cell type-associated node. Later time points (2–4 h, Fig. 5B and D) had increased connectivity (defined as the number of connections for a particular node relative to the total number of nodes in the network) of downstream nodes, particularly NOTCH, OCT4, IRF1, and SNAIL in the $BRCA1^{MT/RES}$ cells and NOTCH and GL1 in the $BRCA1^{WT}$ cells. The nodes are interpreted as involved in

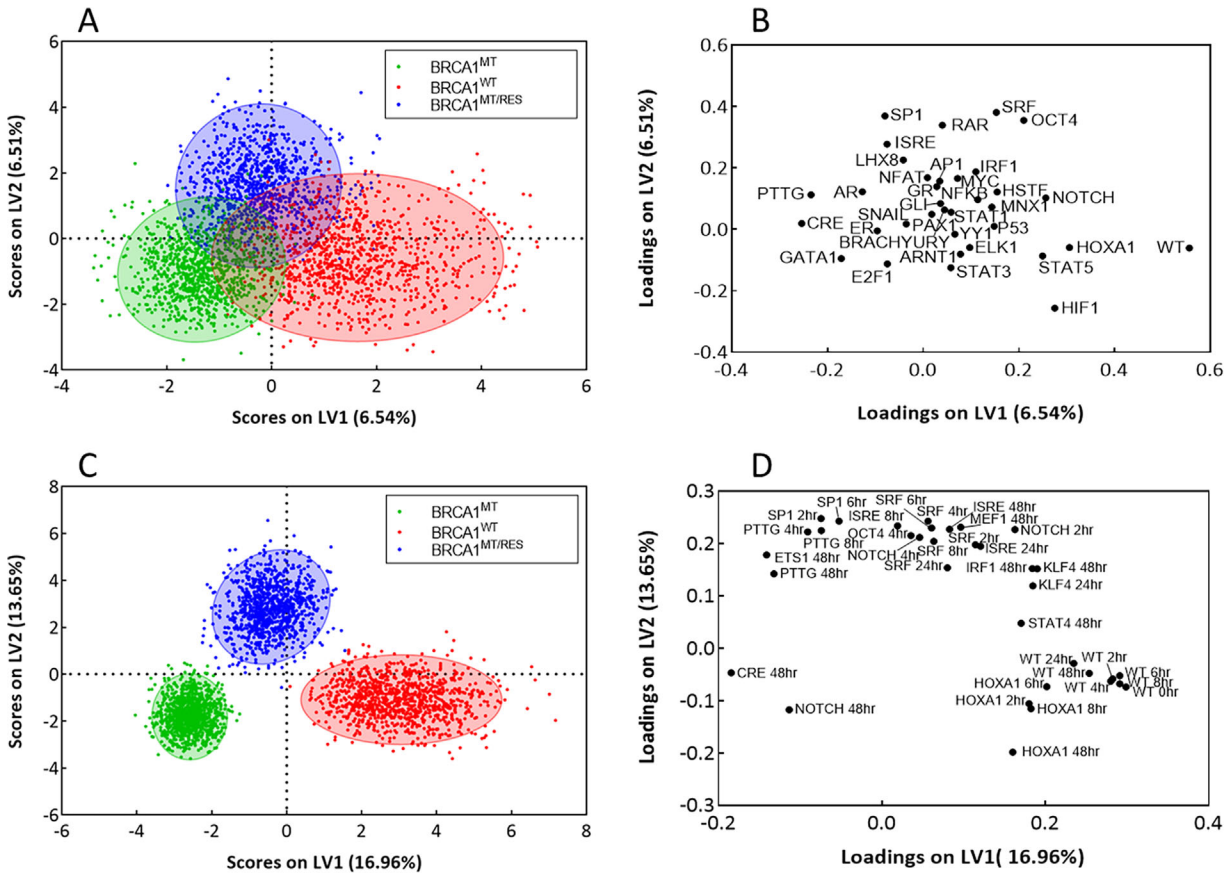

Figure 4. PLSDA analysis of transcription factor activity measurements from BRCA1^{MT} (BRCA1 mutant, green), BRCA1^{WT} (BRCA1 wild-type, red), and BRCA1$^{MT/RES}$ cells (BRCA1 mutant with resistance to Olaparib, blue). Colored regions represent 95% confidence ellipses for each cell type. Specific TF activity patterns associated with each cell group can be identified by the co-localization of the sample scores (A and C) and the TF loadings (B and D). (**A** and **B**) Single time point PLSDA using standardized activity measurements for 35 transcription factors at the was able to separate the three cell groups with 92.0% calibration accuracy and 91.7% cross-validation accuracy. (**C** and **D**) Combined time-course PLSDA using standardized activity measurements for transcription factors at multiple time points after treatment with Olaparib. VIP scores were used to select 35 TF/time point measurements that separate the three cell groups with 99.7% calibration accuracy and 99.7% cross-validation accuracy. The labels on the loadings plot (D) indicate both the name of the transcription factor being used and the elapsed time after the addition of Olaparib.

early response to the drug as they are both downstream of the phenotype and increase in importance with increased treatment duration. Taken together, NOTCH was the only factor that appeared in all inferred networks and was additionally shown to be involved in early response to Olaparib in resistant cell lines.

Inhibition of NOTCH Signaling Sensitized Resistant Cells to Olaparib

The combination of analysis techniques identified NOTCH as a common target in BRCA1^{WT} and BRCA1$^{MT/RES}$ cells to desensitize them to Olaparib treatment. NOTCH protein overexpression in BRCA1^{WT} and BRCA1$^{MT/RES}$ cells was confirmed by Western blot (Fig. 6A). Specifically, NOTCH3 was overexpressed while NOTCH1 expression was consistent between cell types. The direct role of NOTCH signaling in PARP1 inhibitor-induced cell death and the development of resistance was investigated by treating BRCA1^{WT} and BRCA1$^{MT/RES}$ cells with both Olaparib and γ-secretase inhibitor (GSI), which specifically inhibits NOTCH signaling (Fig. 6B). Cell viability decreased for both resistant cell groups during co-treatment, with BRCA1^{WT} cells showing 40% decrease in viability with co-treatment and BRCA1$^{WT/RES}$ cells showing 75% decrease in viability by MTS assay. These results are consistent with our identification of NOTCH activity as an important factor in acquired Olaparib resistance, and they suggest that acquired resistance independent of BRCA1 restoration is distinctly sensitive to NOTCH inhibition in combination with Olaparib.

Discussion

Resistance to PARP inhibitors can proceed through a variety of mechanisms. BRCA can be restored, thus preventing the combination of events that lead to synthetic lethality (Barber et al., 2013). Resistance can also proceed through enhanced drug clearance (Lord and Ashworth, 2013; Rottenberg et al., 2008) or secondary mutations that lead to deletion of the *53bp1* gene, which prevents PARP action at the site of DNA damage (Jaspers et al., 2013). Crucially important are the regulatory factors that can lead to one or a combination of these events. This study identified core transcription factors and pathways that distinguish parental

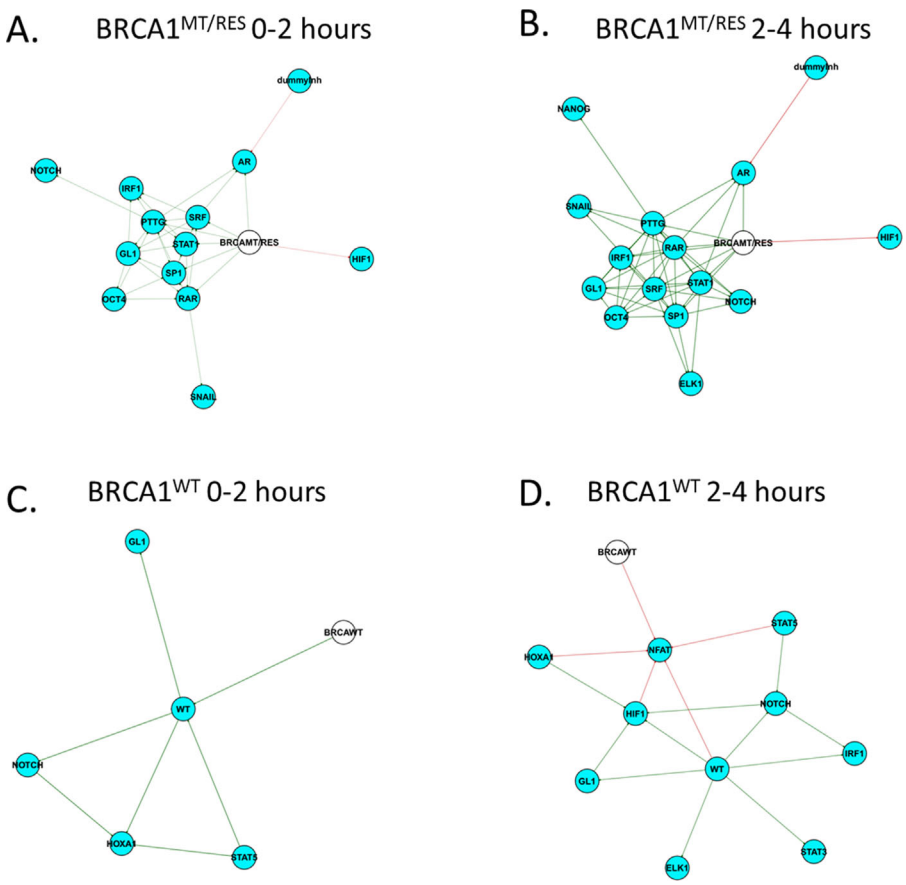

Figure 5. Inferred regulatory networks in BRCA1$^{MT/RES}$ and BRCA1^{WT} cells. Networks depict regulatory interactions relative to BRCA^{MT} cells during the first 4 h of PARPi treatment. White node indicates the cell type. Green edges indicate activating interaction, red edges indicate deactivating interactions. (**A** and **B**) networks for BRCA1RES/MT cells from 0 to 2 and 2 to 4 h. (**C** and **D**) networks for BRCA1WT cells from 0 to 2 and 2 to 4 h.

HCC1937 cells (BRCA^{MT}) from cells with restored BRCA1 (BRCA1^{WT}) and cells with acquired resistance (BRCA1$^{MT/RES}$), using both supervised and unsupervised classification prior to treatment with Olaparib. Because NOTCH was (i) significantly different in the two resistant cell lines compared to the parental line; (ii) in the top 10% of VIP scores via PLSDA on the dynamic TF activity data; and (iii) implicated in the early response to Olaparib by NTRACER, NOTCH inhibition was investigated in combination with Olaparib treatment, and we observed that this combination could overcome resistance.

The association of NOTCH with mutant BRCA1, sensitivity to PARP inhibition, and upregulation following the development of resistance is consistent with the role of NOTCH signaling in breast cancer development. BRCA1 has been reported to upregulate NOTCH signaling by transcriptionally upregulating NOTCH ligands and receptors, which may be important for normal breast tissue differentiation (Buckley et al., 2013). This role of NOTCH during development would be consistent with the observation that BRCA1 mutation may prevent the ability to upregulate NOTCH. In human breast cancer, aberrant activation of NOTCH1 has been observed (Stylianou et al., 2006), and examination of breast cancer patients' clinicopathological parameters reports that a high level of NOTCH1 may be associated with a poorer outlook for the breast cancer patient, while a high level of NOTCH2 correlated to a higher chance of survival (Parr et al., 2004). Herein, we report an association of NOTCH signaling with PARP1 inhibitor-induced breast cancer cell death, which was further validated by demonstration of increased cell death following co-treatment with PARP1 and NOTCH signaling inhibitors for BRCA1 wild-type and mutant cells. Furthermore, PARP1 inhibitor-resistant BRCA1 mutant cells had an increased expression of NOTCH3. NOTCH fusions have been reported in triple negative breast cancer cells, which could provide a means for upregulation of NOTCH activity despite BRCA1 mutation (Robinson et al., 2011), thereby providing resistance to PARP1i treatment. Our results, combined with the increasing evidence supporting the association of NOTCH pathways with breast cancer development, suggest that PARP1 inhibitor-induced cell death and development of resistance might be related to restored NOTCH activity, which is lowered in the BRCA1-mutant cell type.

A key component to identifying NOTCH was the incorporation of dynamic TF activity measurements, which improved the classification accuracy of the models compared with static techniques. The ability of the TRACER platform to capture dynamic changes provides a distinct advantage over comparable techniques based on

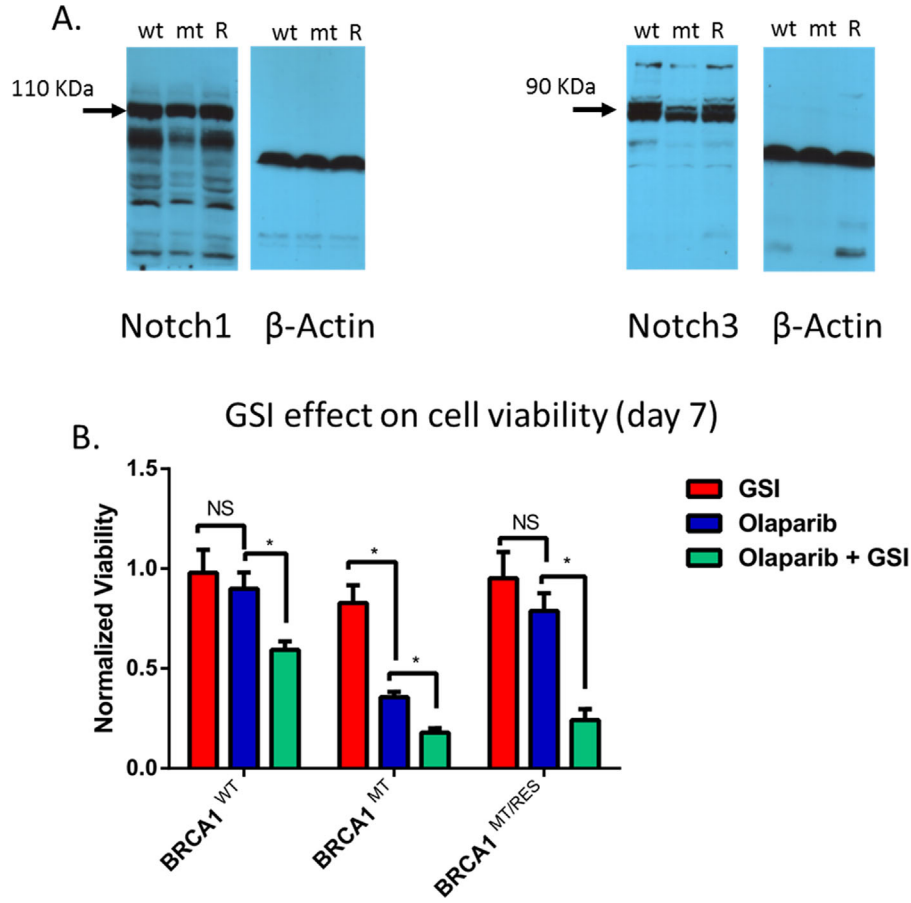

Figure 6. NOTCH signaling is related to PARPi resistance. (**A**) Notch3 protein was elevated in two PARPi resistant cell lines, while Notch1 protein was unchanged. (**B**)Three cell lines ($BRCA^{WT}$, $BRCA^{MT}$, and $BRCA^{MT/RES}$) were treated by 10 μM of Olaparib, 0.5 μM of GSI, and both for 7 days. The values were represented by the MTS ratio to DMSO-treated control. Co-treatment of Olaparib and GSI significantly affected cell viability ($P < 0.01$).

cell lysis and measurements of abundance, where acquiring multiple time points can be prohibitively labor intensive or expensive to perform. By measuring TF activity at multiple time points in the live cell assays, the probable phenotype of the cell was more easily classified, potentially recognizing resistance days before the efficacy of treatment can be assessed. Incorporation of dynamics into the supervised PLSDA model resulted in more than a 10-fold reduction in misclassified points compared to single time point PLSDA. Importantly, 48 h of treatment and measurement were used for classification in this study, which is before a significant response was observed to the drug in sensitivity assays (Fig. 1). Equally important, VIP scores identified NOTCH at 2 h as the top scoring classifier in the model. Latent variable loadings in the combined time-course PLSDA model indicate the association of this early NOTCH response, but not the later response, with the resistant phenotype, which supports the utility of comparing dynamic measurements (Fig. 4). Static measurements would not have identified the complex role of this factor, which ultimately proved important to the development of resistance in the model system (Fig. S3A).

Furthermore, the combination of analysis techniques used in this study was essential to identifying NOTCH as a potential driver of resistance to Olaparib. Statistical analysis is useful for finding factors that are differentially regulated between cell types and different time points of treatment, however, determining the factors ultimately responsible for resistance is difficult to determine. PLSDA was applied in this study to identify differences in the two phenotypes (resistant and sensitive) as well as differences between cells with different mechanisms of resistance. The latent variables generated during PLSDA provide an excellent means for representing multivariate TF activity measurements and a distinct advantage over other classification techniques in visualization and interpretation (Ballabio and Consonni, 2013). PLSDA allowed identification of relationships between TFs (or "signatures") that best differentiated cell phenotypes. Additionally, PLSDA directly complements these baseline statistical measurements by providing a measure of the factors that are "important"; that is, the factors that can be used to identify one cell type from the others, and, through the VIP score, rank, the relative importance of each factor within the model. Network analysis (NTRACER) generated a model of the factors that are directly connected to the phenotype, the factors that are associated with the response to the drug, and how these factors change in importance over time. The network analysis provided a biological context for the PLSDA measurements, in which the role of

a particular factor in the response could be elucidated. In this study, we tested one TF identified as a key hub by our network analysis, yet future studies could use additional TF signatures to design combinatorial therapies.

The techniques used in this study each suggested NOTCH signaling as essential to the response of both resistant cell types, though the analysis suggests $BRCA1^{WT}$ and $BRCA1^{MT/RES}$ have distinct mechanisms of resistance. NOTCH activity is linked to the BRCA1 protein and thus likely the cause of increased NOTCH activity in the $BRCA1^{WT}$ cell line; this would also account for the relative simplicity of the $BRCA1^{WT}$ network, as the response to PARP inhibition would proceed through the BRCA1 protein, which was not measured in these experiments. Conversely, NOTCH signaling was associated with pluripotency markers (OCT4, NANOG) in the $BRCA1^{MT/RES}$ cell lines by both PLSDA and NTRACER. This association of NOTCH with OCT4 and NANOG is consistent with previous reports in which signaling in resistant cancer cells was connected with the cancer stem cell phenotype (Bhola et al., 2016; D'Angelo et al., 2015; Qiu et al., 2013; Reya et al., 2001; Ying et al., 2011). The association of pluripotency markers (OCT4, NANOG) with $BRCA1^{MT/RES}$ cells but not $BRCA1^{WT}$ cells possibly indicates a stem cell phenotype for these cells and that this phenotype may enhance NOTCH activity that contributes to the resistance to Olaparib.

In conclusion, we employed TRACER to report on the activity of numerous TFs in BRCA1-mutated cells during treatment with Olaparib and identified key TFs associated with PARP inhibition. The NOTCH pathway was identified as a key factor in supporting resistance to PARP inhibitor therapy through a combination of techniques. The analysis strategies utilized here could be applied to other cancer/therapy systems to identify pathways important to drug resistance, as well as identify potential mechanisms for drug action on these cells. Furthermore, strategies such as those developed herein to identify NOTCH signaling may also be employed to identify therapeutic targets critical to overcoming resistance to a variety of pharmaceuticals, which is a mounting challenge to the clinical management of advanced cancers.

This work was funded by NIH grant RO1GM097220-05 (J.S.J. and L.D.S.).

References

Arnold KB, Burgener A, Birse K, Romas L, Dunphy LJ, Shahabi K, Abou M, Westmacott GR, McCorrister S, Kwatampora J. 2016. Increased levels of inflammatory cytokines in the female reproductive tract are associated with altered expression of proteases, mucosal barrier proteins, and an influx of HIV-susceptible target cells. Mucosal Immunol 9(1):194–205.

Arnold KB, Szeto GL, Alter G, Irvine DJ, Lauffenburger DA. 2015. CD4+ T cell-dependent and CD4+ T cell-independent cytokine-chemokine network changes in the immune responses of HIV-infected individuals. Sci Signal 8(399):ra104.

Ballabio D, Consonni V. 2013. Classification tools in chemistry. Part 1: Linear models. PLS-DA. Anal Methods 5(16):3790–3798.

Barber LJ, Sandhu S, Chen L, Campbell J, Kozarewa I, Fenwick K, Assiotis I, Rodrigues DN, Reis-Filho JS, Moreno V. 2013. Secondary mutations in BRCA2 associated with clinical resistance to a PARP inhibitor. J Pathol 229(3):422–429.

Benedict KF, Lauffenburger DA. 2012. Insights into proteomic immune cell signaling and communication via data-driven modeling. Systems Biology: Springer Heidelberg, Germany. p 201–233.

Benjamini Y, Hochberg Y. 1995. Controlling the false discovery rate: A practical and powerful approach to multiple testing. J R Stat Soc Series B Methodol 57:289–300.

Bernabé BP, Shin S, Rios PD, Broadbelt LJ, Shea LD, Seidlits SK. 2016. Dynamic transcription factor activity networks in response to independently altered mechanical and adhesive microenvironmental cues. Integr Biol. 8(8):844–860.

Beste MT, Pfäffle-Doyle N, Prentice EA, Morris SN, Lauffenburger DA, Isaacson KB, Griffith LG. 2014. Molecular network analysis of endometriosis reveals a role for c-Jun-regulated macrophage activation. Sci Transl Med 6(222):222ra16.

Bhola NE, Jansen VM, Koch JP, Li H, Formisano L, Williams JA, Grandis JR, Arteaga CL. 2016. Treatment of triple-negative breast cancer with TORC1/2 inhibitors sustains a drug-resistant and notch-dependent cancer stem cell population. Cancer Res 76(2):440–452.

Breiman L. 2001. Random forests. Mach Learn 45(1):5–32.

Bryant HE, Schultz N, Thomas HD, Parker KM, Flower D, Lopez E, Kyle S, Meuth M, Curtin NJ, Helleday T. 2005. Specific killing of BRCA2-deficient tumours with inhibitors of poly (ADP-ribose) polymerase. Nature 434(7035):913–917.

Buckley NE, Nic An tSaoir CB, Blayney JK, Oram LC, Crawford NT, D'Costa ZC, Quinn JE, Kennedy RD, Harkin DP, Mullan PB. 2013. BRCA1 is a key regulator of breast differentiation through activation of Notch signalling with implications for anti-endocrine treatment of breast cancers. Nucleic Acids Res 41(18):8601–8614.

Buege M, Mahajan PB. 2015. Clinical trials of poly (ADP-ribose) polymerase inhibitors for cancer therapy: A review. Rev Recent Clin Trials 10(4):326–339.

Chong I-G, Jun C-H. 2005. Performance of some variable selection methods when multicollinearity is present. Chemometr Intell Lab Syst 78(1):103–112.

Csardi G, Nepusz T. 2006. The igraph software package for complex network research. InterJournal Complex Syst 1695(5):1–9.

D'Angelo RC, Ouzounova M, Davis A, Choi D, Tchuenkam SM, Kim G, Luther T, Quraishi AA, Senbabaoglu Y, Conley SJ. 2015. Notch reporter activity in breast cancer cell lines identifies a subset of cells with stem cell activity. Mol Cancer Ther 14(3):779–787.

Dull T, Zufferey R, Kelly M, Mandel R, Nguyen M, Trono D, Naldini L. 1998. A third-generation lentivirus vector with a conditional packaging system. J Virol 72(11):8463–8471.

Faith JJ, Hayete B, Thaden JT, Mogno I, Wierzbowski J, Cottarel G, Kasif S, Collins JJ, Gardner TS. 2007. Large-scale mapping and validation of *Escherichia coli* transcriptional regulation from a compendium of expression profiles. PLoS Biol 5(1):e8.

Farmer H, McCabe N, Lord CJ, Tutt AN, Johnson DA, Richardson TB, Santarosa M, Dillon KJ, Hickson I, Knights C. 2005. Targeting the DNA repair defect in BRCA mutant cells as a therapeutic strategy. Nature 434(7035):917–921.

Ford D, Easton DF, Bishop DT, Narod SA, Goldgar DE. 1994. Risks of cancer in BRCA1-mutation carriers. Breast cancer linkage consortium. Lancet 343(8899):692–695.

Foulkes WD, Smith IE, Reis-Filho JS. 2010. Triple-negative breast cancer. N Engl J Med 363(20):1938–1948.

Gelmon KA, Tischkowitz M, Mackay H, Swenerton K, Robidoux A, Tonkin K, Hirte H, Huntsman D, Clemons M, Gilks B. 2011. Olaparib in patients with recurrent high-grade serous or poorly differentiated ovarian carcinoma or triple-negative breast cancer: A phase 2, multicentre, open-label, non-randomised study. Lancet Oncol 12(9):852–861.

Haury A-C, Mordelet F, Vera-Licona P, Vert J-P. 2012. TIGRESS: Trustful inference of gene regulation using stability selection. BMC Syst Biol 6(1):1.

Henneman L, van Miltenburg MH, Michalak EM, Braumuller TM, Jaspers JE, Drenth AP, de Korte-Grimmerink R, Gogola E, Szuhai K, Schlicker A. 2015. Selective resistance to the PARP inhibitor olaparib in a mouse model for BRCA1-deficient metaplastic breast cancer. Proc Natl Acad Sci USA 112(27): 8409–8414.

Jaspers JE, Kersbergen A, Boon U, Sol W, van Deemter L, Zander SA, Drost R, Wientjens E, Ji J, Aly A. 2013. Loss of 53BP1 causes PARP inhibitor resistance in Brca1-mutated mouse mammary tumors. Cancer Discov 3(1):68–81.

Johnson N, Johnson SF, Yao W, Li Y-C, Choi Y-E, Bernhardy AJ, Wang Y, Capelletti M, Sarosiek KA, Moreau LA. 2013. Stabilization of mutant BRCA1 protein confers PARP inhibitor and platinum resistance. Proc Natl Acad Sci USA 110(42):17041–17046.

Kim G, Ison G, McKee AE, Zhang H, Tang S, Gwise T, Sridhara R, Lee E, Tzou A, Philip R. 2015. FDA approval summary: Olaparib monotherapy in patients with deleterious germline BRCA-mutated advanced ovarian cancer treated with three or more lines of chemotherapy. Clin Cancer Res 21(19):4257–4261.

King M-C, Marks JH, Mandell JB. 2003. Breast and ovarian cancer risks due to inherited mutations in BRCA1 and BRCA2. Science 302(5645):643–646.

Ledermann J, Harter P, Gourley C, Friedlander M, Vergote I, Rustin G, Scott C, Meier W, Shapira-Frommer R, Safra T. 2012. Olaparib maintenance therapy in platinum-sensitive relapsed ovarian cancer. N Engl J Med 366(15):1382–1392.

Lord CJ, Ashworth A. 2013. Mechanisms of resistance to therapies targeting BRCA-mutant cancers. Nat Med 19(11):1381–1388.

Lord CJ, Tutt AN, Ashworth A. 2015. Synthetic lethality and cancer therapy: Lessons learned from the development of PARP inhibitors. Annu Rev Med 66:455–470.

Margolin AA, Nemenman I, Basso K, Wiggins C, Stolovitzky G, Favera RD, Califano A. 2006. ARACNE: An algorithm for the reconstruction of gene regulatory networks in a mammalian cellular context. BMC Bioinformatics 7(Suppl 1):S7.

Mevik B-H, Wehrens R. 2007. The pls package: Principal component and partial least squares regression in R. J Stat Software 18(2):1–24.

Meyer PE, Kontos K, Lafitte F, Bontempi G. 2007. Information-theoretic inference of large transcriptional regulatory networks. EURASIP J Bioinform Syst Biol 2007(1):1–9.

Parr C, Watkins G, Jiang W. 2004. The possible correlation of Notch-1 and Notch-2 with clinical outcome and tumour clinicopathological parameters in human breast cancer. Int J Mol Med 14:779–786.

Qiu M, Peng Q, Jiang I, Carroll C, Han G, Rymer I, Lippincott J, Zachwieja J, Gajiwala K, Kraynov E. 2013. Specific inhibition of Notch1 signaling enhances the antitumor efficacy of chemotherapy in triple negative breast cancer through reduction of cancer stem cells. Cancer Lett 328(2):261–270.

Reis-Filho J, Tutt A. 2008. Triple negative tumours: A critical review. Histopathology 52(1):108–118.

Reya T, Morrison SJ, Clarke MF, Weissman IL. 2001. Stem cells, cancer, and cancer stem cells. Nature 414(6859):105–111.

Robinson DR, Kalyana-Sundaram S, Wu YM, Shankar S, Cao X, Ateeq B, Asangani IA, Iyer M, Maher CA, Grasso CS, Lonigro RJ. 2011. Functionally recurrent rearrangements of the MAST kinase and Notch gene families in breast cancer. Nat Med 17(12):1646–1651.

Rottenberg S, Jaspers JE, Kersbergen A, van der Burg E, Nygren AO, Zander SA, Derksen PW, de Bruin M, Zevenhoven J, Lau A. 2008. High sensitivity of BRCA1-deficient mammary tumors to the PARP inhibitor AZD2281 alone and in combination with platinum drugs. Proc Natl Acad Sci USA 105(44): 17079–17084.

Rouleau M, Patel A, Hendzel MJ, Kaufmann SH, Poirier GG. 2010. PARP inhibition: PARP1 and beyond. Nat Rev Cancer 10(4):293–301.

Siletz A, Schnabel M, Kniazeva E, Schumacher AJ, Shin S, Jeruss JS, Shea LD. 2013. Dynamic transcription factor networks in epithelial-mesenchymal transition in breast cancer models. PLoS ONE 8(4):e57180.

Smyth GK. 2005. Limma: Linear models for microarray data. Bioinformatics and computational biology solutions using R and bioconductor. New York, NY: Springer. p 397–420.

Stylianou S, Clarke RB, Brennan K. 2006. Aberrant activation of notch signaling in human breast cancer. Cancer Res 66(3):1517–1525.

Terfve C, Cokelaer T, Henriques D, MacNamara A, Goncalves E, Morris MK, van Iersel M, Lauffenburger DA, Saez-Rodriguez J. 2012. CellNOptR: A flexible toolkit to train protein signaling networks to data using multiple logic formalisms. BMC Syst Biol 6(1):1.

Tutt A, Robson M, Garber J, Domchek S, Audeh M, Weitzel J, Friedlander M, Carmichael J. 2009. Phase II trial of the oral PARP inhibitor olaparib in BRCA-deficient advanced breast cancer. J Clin Oncol 27(18):p CRA501.

Weiss M, Bernabé BP, Shin S, Asztalos S, Dubbury S, Mui M, Bellis A, Bluver D, Tonetti D, Saez-Rodriguez J, Broadbelt LJ, Jeruss JS, Shea LD. 2014. Dynamic transcription factor activity and networks during ErbB2 breast oncogenesis and targeted therapy. Integr Biol 6(12):1170–1182.

Westerhuis JA, Hoefsloot HC, Smit S, Vis DJ, Smilde AK, van Velzen EJ, van Duijnhoven JP, van Dorsten FA. 2008. Assessment of PLSDA cross validation. Metabolomics 4(1):81–89.

Ying M, Wang S, Sang Y, Sun P, Lal B, Goodwin C, Guerrero-Cazares H, Quinones-Hinojosa A, Laterra J, Xia S. 2011. Regulation of glioblastoma stem cells by retinoic acid: Role for Notch pathway inhibition. Oncogene 30(31):3454–3467.

Supporting Information

Additional supporting information may be found in the online version of this article at the publisher's web-site.